Phytochemistry 183 (2021) 112598

Contents lists available at ScienceDirect

Phytochemistry

journal homepage: www.elsevier.com/locate/phytochem

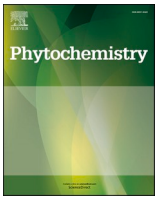

Biotransformation of papaverine and in silico docking studies of the metabolites on human phosphodiesterase 10a

Duaa Eliwa [a,b], Mohamed A. Albadry [a], Abdel-Rahim S. Ibrahim [b], Amal Kabbash [b], Kumudini Meepagala [c], Ikhlas A. Khan [a,d], Mona El-Aasr [b], Samir A. Ross [a,d,*]

[a] National Center for Natural Products Research, School of Pharmacy, The University of Mississippi, MS, 38677, USA
[b] Department of Pharmacognosy, Faculty of Pharmacy, Tanta University, Tanta, 31527, Egypt
[c] USDA-ARS, Natural Products Utilization Research Unit, University, MS, USA
[d] Division of Pharmacognosy, Department of Biomolecular Sciences, School of Pharmacy, University of Mississippi, MS, 38677, USA

ARTICLE INFO

Keywords:
Biotransformation
Benzylisoquinoline alkaloids
Papaverine
Aspergillus niger NRRL 322
Beauveria bassiana NRRL 22864
Cunninghamella echinulate ATCC 18968
Cunninghamella echinulate ATCC 1382
Human phosphodiesterase 10a
Molecular docking

ABSTRACT

The metabolism of papaverine, the opium benzylisoquinoline alkaloid, with *Aspergillus niger* NRRL 322, *Beauveria bassiana* NRRL 22864, *Cunninghamella echinulate* ATCC 18968 and *Cunninghamella echinulate* ATCC 1382 has resulted in O-demethylation, O-methylglucosylation and N-oxidation products. Two new metabolites (4″-O-methyl-β-D-glucopyranosyl) 4′-demethyl papaverine and (4″-O-methyl-β-*D*-glucopyranosyl) 6-demethyl papaverine, (Metabolites **5** and **6)** together with 4′-O-demethylated papaverine (Metabolite **1)**, 3′-O-demethylated papaverine (Metabolite **2**), 6-O-demethylated papaverine (Metabolite **3)** and papaverine N-oxide (Metabolite **4)** were isolated. The structure elucidation of the metabolites was based primarily on 1D, 2D-NMR analyses and HRMS. These metabolism results were consistent with the previous plant cell transformation studies on papaverine and isopapaverine and the microbial metabolism of papaveraldine. In silico docking studies of the metabolites using crystals of human phosphodiesterase 10a (hPDE10a) revealed that compounds **4**, **1**, **6**, **3**, and **5** possess better docking scores and binding poses with favorable interactions than the native ligand papaverine.

1. Introduction

Biotransformations (bioconversion or microbial transformation) refer to the processes in which microorganisms convert organic compounds into structurally related products. In other word, biotransformation deals with microbial (enzymatic) conversion of a substrate into a product with limited number (one or few) enzymatic reactions (Hegazy et al., 2015). The microbial transformation of natural and synthetic drugs has been extensively used to decipher the fate of therapeutic agents in the body, prepare novel drugs, and mediate preparation of synthetic drugs. The microbial reactions are characterized by being highly stereoselective and regioselective (Veeresham and Venisetty, 2003). The 1-benzylisoquinoline papaverine is a major alkaloid in the latex of opium poppy chemo types and has been used as a non-specific vasodilator owing to its direct action on smooth muscle (Facchini and Hagel, 2013). Although its use to treat cerebral vasospasm has largely been replaced by modern drugs, papaverine is still used topically and as an injectable to treat erectile dysfunction (Facchini and Hagel, 2013). A cell cultures of *Silene alba* Miller was able to transform papaverine to papaveraldine (Dorisse et al., 1986). *Silene alba* Miller E. H. L. Krause cell suspension also transformed papaverine to 6- and 4′-monodemethylpapaverine (Verdeil et al., 1986). Also, *Mucor ramannianus* 1839 was able to transform papaveraldine into *S*-papaverinol and *S*-papaverinol N-oxide (El Sayed, 2000). Four metabolites were separated from rat bile treated with papaverine which are 4′-desmethyl-, 7-desmethyl-, and 6-desmethylpapaverine and 4′,6- desmethylpapaverine (Belpaire et al., 1975). Papaverine is a selective inhibitor of Phosphodiesterase 10. Phosphodiesterase 10 (PDE10) is a dual-specificity superfamily responsible for hydrolyzing both cAMP (Km = 0.05 μM) and cGMP (Km = 3 μM) (Li et al., 2018), which is highly expressed in the brain and has been considered as a potential target for the treatment of several central nervous system (CNS) disorders such as Schizophrenia, Huntington's and psychiatric disorders that affect the basal ganglia disease (Lee et al., 2019). In recent study PDE10A had a unique role in the development of heart failure and pathological cardiac remodeling (Chen et al., 2020). Taking into consideration that inhibition of PDE10A might represent a novel therapeutic strategy for treating wide array of diseases associated with CNS and the cardiovascular system, we used the

* Corresponding author. National Center for Natural Products Research, School of Pharmacy, The University of Mississippi, MS, 38677, USA.
E-mail address: sross@olemiss.edu (S.A. Ross).

https://doi.org/10.1016/j.phytochem.2020.112598
Received 17 August 2020; Received in revised form 20 November 2020; Accepted 24 November 2020
Available online 25 December 2020

Table 1
^{1}H NMR (400 MHz) spectroscopic data for Papaverine, metabolites 1 and 4 (in $CDCl_3$) and metabolites 2, 3, **5** and **6** (in DMSO-d_6)[a].

Position	papaverine	δ_H (multiplicities, *J* in Hz)					
		1	2	3	4	5	6
3	8.33, *d* (5.6)	8.29,*d* (5.5)	8.17, *d* (5.7)	8.38, *d* (5.6)	8.33, *d* (6.1)	8.24, *d* (5.7)	8.31, *d* (6.1)
4	7.53, *d* (5.7)	7.42, *d* (5.5)	7.42, *d* (5.7)	7.63, *d* (5.7)	7.83, *d* (6.1)	7.48, *d* (5.6)	7.87, *d* (6.1)
5	7.01, *s*	7.02, *s*	7.14, *s*	7.74, *s*	7.23, *s*	7.45, *s*	7.55, *s*
8	7.41, *s*	7.35, *s*	7.52, *s*	7.83, *s*	7.60, *s*	7.54, *s*	7.72, *s*
2′	6.94, *d* (1.8)	6.77, *d* (2)	7.00, *d* (2)	7.05, *d* (1.8)	7.29, brs	7.00, *d* (1.8)	7.19, *d* (1.6)
5′	6.74, brs	6.76, brs	6.803, brs	6.80, brs	6.80, brs	6.79, *d* (8.2)	6.95, d (8.5)
6′	6.82, *m*	6.74, *m*	6.800, *brs*	6.81, *m*	6.82, *m*	6.74, *dd* (8.2, 1.9)	6.82, *dd (8.5, 1.6)*
α	4.56, *s*	4.52, *s*	4.47, *s*	4.56, *s*	4.91, *s*	4.48, *s*	4.71, *s*
6-OMe	4.02, *s*	3.97, *s*	_	3.93, *s*	4.10, *s*	_	3.97, *s*
7-OMe	3.93, *s*	3.87, *s*	3.89, *s*	3.86, *s*	4.02, *s*	3.87, *s*	3.94, *s*
3′-OMe	3.78, *s*	3.65, *s*	3.66, *s*	3.67, *s*	_	3.66, *s*	3.72, *s*
4′-OMe	3.80, *s*	_	3.68, *s*	3.69, *s*	3.87, *s*	3.67, *s*	_
1″	_	_	_	_	_	5.17, *d* (7.89)	4.82, *d* (7.76)
2″	_	_	_	_	_	3.41 (*m*)	3.41 (*m*)
3″	_	_	_	_	_	3.46 (*m*)	3.46 (*m*)
4″	_	_	_	_	_	3.04 (*t*, 9.0)	3.02 (*t*, 9.0)
5″	_	_	_	_	_	3.48 (*m*)	3.48 (*m*)
6″	_	_	_	_	_	3.55 (brd, 5.9)	3.55 (brd, 5.9)
4″-OMe	_	_	_	_	_	3.46, *s*	3.43, *s*

Table 2
^{13}C NMR (100 MHz) spectroscopic data for Papaverine, metabolites 1 and 4 (in $CDCl_3$) and metabolites 2, 3, **5** and **6** (in DMSO-d_6)[a].

Position	Papaverine	δ_H (multiplicities, *J*)					
		1	2	3	4	5	6
1	156.9, C	157.8, C	157.7, C	158.9, C	154.0, C	158.5, C	156.2, C
3	139.0, CH	139.8, CH	139.7, CH	140.8, CH	129.5, CH	140.9, CH	134.8, CH
4	119.6, CH	119.4, CH	120.6, CH	120.6, CH	121.0, CH	121.0, CH	119.9, CH
4a	134.6, C	134.1, C	133.3, C	131.8, C	136.8, C	132.9, C	135.5, C
5	105.6, CH	105.6, CH	108.7, CH	119.6, CH	105.7, CH	109.5, CH	106.7, CH
6	150.7, C	153.2, C	147.2, C	152.8, C	156.8, C	150.1, C	155.20, C
7	149.3, C	150.4, C	150.9, C	150.4, C	152.4, C	149.0, C	151.5, C
8	104.5, CH	104.7, CH	104.7, CH	106.1, CH	104.7, CH	105.3, CH	105.3, CH
8a	122.9, C	123.2, C	127.8, C	125.4, C	122.3, C	125.1, C	122.4, C
1′	131.6, C	131.1, C	132.2, C	131.4, C	127.0, C	132.7, C	131.7, C
2′	111.3, CH	111.7, CH	112.7, CH	112.7, CH	114.2, CH	113.1, CH	113.7, CH
3′	147.9, C	147.4, C	149.5, C	147.2, C	145.0, C	147.6, C	149.3, C
4′	149.3, C	144.9, C	148.6, C	148.6, C	147.1, C	147.7, C	145.6, C
5′	112.2, CH	114.9, CH	111.9, CH	111.9, CH	112.0, CH	112.3, CH	115.8, CH
6′	120.7, CH	121.4, CH	117.9, CH	119.0, CH	121.3, CH	119.1, CH	121.2, CH
α	40.6, CH_2	41.8, CH_2	40.6, CH_2	40.9, CH_2	36.6, CH_2	41.2, CH_2	38.3, CH_2
6-OMe	55.9, CH_3	56.1, CH_3	–	55.40, CH_3	56.7, CH_3	–	56.7, CH_3
7-OMe	56.1, CH_3	56.2, CH_3	55.4, CH_3	55.43, CH_3	56.3, CH_3	55.8, CH_3	56.6 CH_3
3′-OMe	56.1, CH_3	56.4, CH_3	55.5, CH_3	55.9, CH_3	–	55.9, CH_3	56.1, CH_3
4′-OMe	56.4, CH_3	–	55.7, CH_3	56.3, CH_3	56.2, CH_3	56.1, CH_3	–
1″	–	–	–	–	–	99.6, CH	100.1, CH
2″	–	–	–	–	–	73.7, CH	73.8, CH
3″	–	–	–	–	–	76.1, CH	75.9, CH
4″	–	–	–	–	–	79.2, CH	79.4, CH
5″	–	–	–	–	–	77.0, CH	76.9, CH
6″	–	–	–	–	–	60.5, CH_2	60.6, CH_2
4″-OMe	–	–	–	–	–	60.2, CH_3	60.1, CH_3

[a] Carbon multiplicity were determined by DEPTq experiment.

microbial biotransformation to generate some papaverine related products followed by molecular docking studies using the Schrodinger software to analyze and understand the binding patterns of these compounds with PDE10.

The use of microbial synthesis can, in many cases, reduces delivery times, minimize resources required, and circumvent speculative chemical synthesis (Salter et al., 2019).

2. Results and discussion

2.1. The biotransformation products identification

Seventy-two strains of filamentous fungi of different classes were used in the initial screening of papaverine. Six metabolites of papaverine were isolated from the biotransformation broth and freeze–dried mycelia of *Aspergillus niger* NRRL 322, *Beauveria bassiana* NRRL 22864, *Cunninghamella echinulate* ATCC 18968 and *Cunninghamella echinulate* ATCC 1382. The metabolites were identified on the basis of their mass and NMR spectroscopic data (Table 1 and Table 2).

The molecular formula of **1** was established as $C_{19}H_{19}NO_4$ by HR-ESI-MS (SI: S7) analysis which exhibited a protonated molecular ion peak at (*m/z* 326.1487 $[M+H]^+$, calculated for $C_{19}H_{20}NO_4$ which is less than papaverine by 14 Da suggesting a demethylation product. When comparing to the papaverine, the absence of 4′-methoxy group was noticed in the ^{1}H NMR (Table 1, SI: S1, SI: S2). Three methoxy groups resonating at δ_H 3.65, 3.87 and 3.97 and assigned to 3′, 7 and 6 methoxy

Table 3
Structure of papaverine and its metabolites.

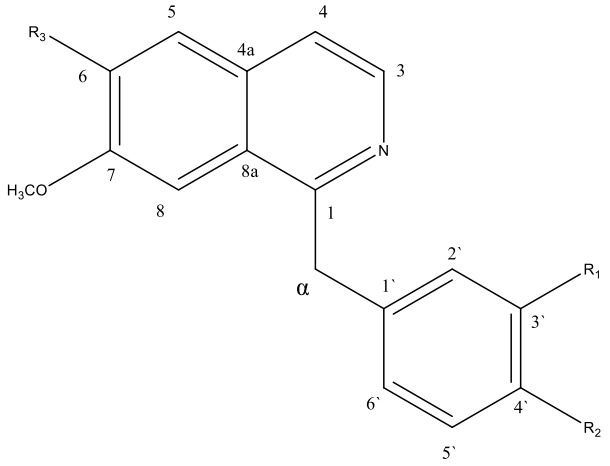

	R_1	R_2	R_3
Papaverine	OCH_3	OCH_3	OCH_3
1	OCH_3	OH	OCH_3
2	OCH_3	OCH_3	OH
3	OCH_3	OCH_3	OCH_3, N-oxide
4	OH	OCH_3	OCH_3
5	OCH_3	OCH_3	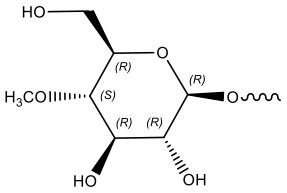
6	OCH_3	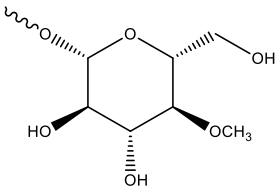	OCH_3

groups, respectively. ^{13}C NMR (Table 2, SI: S3, SI: S4) of **1** showed three methoxy groups signals at 56.1, 56.2 and 56.4 ppm which is less than papaverine by one methoxy and C-4′ signal was further deshielded by 4 ppm due to effect of the produced hydroxyl group. This assumption was supported by detailed analysis of the HMBC and HSQC spectra of **1**(SI: S5, SI: S6).

All data were consistent with those reported for the 4′-O-demethylated product and identical to those reported spectra for 4′-demethylpapaverine(Brochmann-Hanssen, Brochmann-Hanssen, Hirai and Hirai, 1968) (Fig. 3, Tables 1 and 3).

The molecular formula of **2** was established as $C_{19}H_{19}NO_4$ by HRMS (SI: S12) analysis which exhibited a protonated molecular ion peak at (*m/z* 326.1424 $[M+H]^+$, calculated for $C_{19}H_{20}NO_4$, which is less than papaverine by 14 Da suggesting demethylation. When comparing to the papaverine, the absence of 6-methoxy group was observed in the ^{1}H NMR (Table 1, SI: S8, SI: S9). Three methoxy groups resonated at δ_H 3.66, 3.68 and 3.89 which were assigned to 3′, 4′ and 7 methoxy groups, respectively. ^{13}C NMR (Table 2, SI: S9) of **2** showed three methoxy group signals at 55.4, 55.5 and 55.7 ppm which is less than papaverine by one methoxy and C-6 signal deshielded by 2 ppm due to the produced hydroxyl group. This assumption was supported by detailed analysis of the HMBC and HSQC spectra of **2** (SI: S10, SI: S11).

All data were consistent with that reported for the 6-O-demethylated product and identical to those reported for 6-O-demethyl-papaverine (Brochmann-Hanssen et al., 1968), (Fig. 3 & Table 3).

The HRMS analysis (SI: S19) of **3** displayed a protonated molecular ion peak $[M+H]^+$ at m/z 356.1601, suggesting the same molecular formula of papaverine with one additional oxygen atom ($C_{20}H_{21}O_5N$). The ^{13}C and ^{1}H-NMR spectra of **3** (Table 1, Table 2, SI: S13, SI: S14, SI: S15, SI: S16) were closely related to those of papaverine and suggested that **3** is the N-oxide derivative of papaverine. The two proton doublets resonated at δ_H 8.38 and 7.63, $J = 5.7$ Hz was assigned to H-3 and H-4, respectively (Table 1) was shifted by δ_{H+}0.05 and – 0.1 ppm, respectively as compared to those of papaverine. The shifting of C-1 and C-3 in **3** (δ C 2.0 and δ C 1.8 ppm, respectively) as compared to those of papaverine was consistent with the fact that metabolite-**3** is the N- oxide derivative of papaverine. This assumption was supported by detailed analysis of the HMBC and HSQC spectra of **3** (SI: S17, SI: S18, Fig. 3, Table 3).

The molecular formula of **4** was established as $C_{19}H_{19}NO_4$ by HRMS analysis (SI: S25) which exhibited a protonated molecular ion peak at (*m/z* 326.1498 $[M+H]^+$, calculated for $C_{19}H_{20}NO_4$ which is less than papaverine by 14 Da suggesting a demethylation. Also, when comparing to the papaverine, the absence of 3′-methoxy group was noticed in the ^{1}H NMR (Table 1, SI: S20, SI: S21). Three methoxy groups were observed at δ_H 3.87, 4.02 and 4.10 ppm which were assigned to 3′, 7 and 6

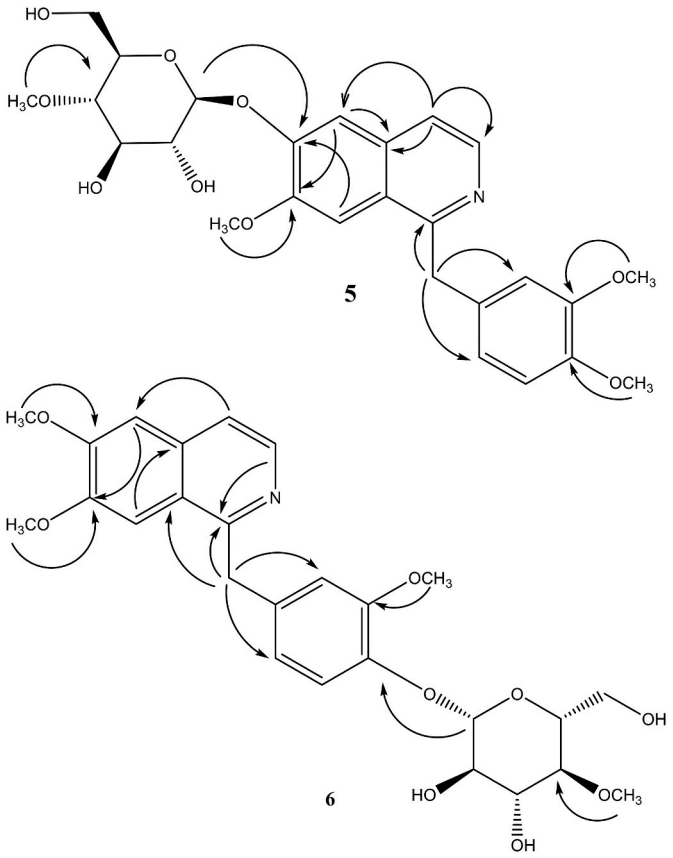

Fig. 1. Important ^{1}H–^{13}C-HMBC correlations of metabolites 5 and 6.

methoxy groups, respectively. ^{13}C NMR of **4** (Table 2, SI: S2) showed three methoxy groups signals at δ 56.2, 56.7 and 56.3 ppm which is less than papaverine by one methoxy and C-3′ signal deshielded by 3 ppm due to the produced hydroxyl group. This assumption was supported by detailed analysis of the HMBC and HSQC spectra of **4**. Hence, **4** was approved as 3′-O-demethyl-papaverine (Brochmann-Hanssen and Hirai, 1968), (SI: S23, SI: S24, Figs. 1 and 3, Table 3).

Metabolite **5** exhibited a protonated molecular ion peak at *m/z* 502.1980 $[M+H]^+$ in its high-resolution ESI-MS(SI: S31), suggesting a molecular formula of $C_{26}H_{32}NO_9$. The molecular weight was the sum of O-demethyl papaverine (325) and an additional moiety of 176 mass units (consistent with O-methyl glucose). Spectroscopic data for this compound were very similar to those of 2 **(**6-O-demethyl-papaverine) and suggested that a 4-O-methylglucose moiety was introduced during the biotransformation (Table 1, Table 2, SI: S26, SI: S27). This was further confirmed by the presence of sugar signals at δ 99.6, 79.2, 77.0, 76.1, 73.7, 60.5 and 60.2 in its ^{13}C NMR spectrum (Table 2, SI: S28). The HMBC correlations of H-1″ (the anomeric protons) to C-6 suggested that the newly introduced 4-O-methylglucose moiety is linked to the isoquinoline moiety at C-6 through an oxygen atom. The anomeric proton resonates at δ 5.17, shows large coupling constant, $J = 7.9$ Hz indicating the aglycone binds to the sugar through a β-glycosidic linkage. Based on the detailed analysis of HSQC and HMBC spectra (Fig. 1), this biotransformation product was identified as (4″-O-methyl-β-D-glucopyranosyl) 6-demethyl papaverine (Figs. 1 and 3, Table 3, SI: S29, SI: S30).

Metabolite **6** had the same molecular formula as **5**. In its ^{1}H NMR and ^{13}C NMR spectra (Table 1, Table 2, SI: S32, SI: S33, SI: S34), the Spectroscopic data for this compound were very similar to those of 1 **(**4-O-demethyl-papaverine) and suggested that a 4-O-methylglucose moiety was introduced during the biotransformation. The presence of a 4-O-methylglucose moiety in this metabolite was confirmed by the occurrence of five methine carbon (CH) signals at δ 100.1, 79.4, 76.9, 75.9, and 73.8, one methylene carbon (CH_2) signal at δ 60.6 and one OCH_3 signal at δ 60.1 in its ^{13}C NMR spectrum (Table 2). The HMBC (Fig. 1, SI: S36) correlations of H-1″ (the anomeric protons) to C-4′ confirmed the attachment of the sugar moiety to C-4′ of metabolite **6**. The high *J* value of the anomeric proton H-1″ suggested the presence of a β-glycosidic linkage in 4′. Metabolite **6** exhibited a peak due to $[M+H]^+$ at m/z 502.2138 in its high-resolution ESI-MS (SI: S37), suggesting a molecular formula of $C_{26}H_{32}NO_9$. Thus, this metabolite was identified as (4″-O-methyl-β-D-glucopyranosyl) 4′-demethyl papaverine (Figs. 1 and 3, Table 3).

2.2. *In silico molecular docking study of the biotransformation products on human phosphodiesterase 10a (HPDE10a)*

Crystal structure of Human PDE-papaverine complex 2WEY(Andersen et al., 2009) et al., 2009), was utilized for the docking study, in which papaverine interacts with the receptor via hydrogen-bonding interaction between the methoxy groups of the isoquinoline moiety with Gln726 in addition to stacking interactions between the isoquinoline group and phenylalanine at positions 696 and 729. Docking was performed using papaverine and compounds (1–6) after ligand preparation step which generated 13 ligands from the input of 7 compounds. In order to obtain a good sampling of the conformational space of these ligands, we performed conformational search using Macromodel. We obtained 2305 total entry as a result 105 for (1) 251 for (2) 183 for (3) 180 for (4) 552 for (5) 666 for (6) 368 for papaverine, the lowest energy conformer of each compound are shown in (Table 4). The output of docking study revealed that several compounds possessed good binding poses with favorable protein-ligand interactions (Fig. 2). A study of the binding modes and the docking scores revealed that five compounds (**4**, **1**, **6, 3**, and **5**) possess better docking scores and binding poses with favorable interactions than the native ligand papaverine (Table 5).

3. Experimental

3.1. *General experimental procedure*

1D (^{1}H, ^{13}C and DEPTQ) and 2D (HMBC and HSQC) NMR spectra were recorded on a Bruker model AMX 400 NMR spectrometer with standard pulse sequences, operating at 400 MHz in ^{1}H and 100 MHz in ^{13}C. The chemical shift (δ) values were reported in parts per million units (ppm) and tetramethylsilane or known solvent shifts, used as internal chemical shift references. Coupling constants (*J* values) were recorded in Hertz (Hz). Standard pulse sequences were used for COSY, HSQC, HMBC, and DEPT. High-resolution electrospray ionization mass spectra (ESI-MS) were measured on a Micromass Q-T of Micro mass spectrometer with a lock spray source. TLC was performed using precoated TLC sheets silica gel G 254 F sheets (E. Merck, Germany) and precoated C18–W silica TLC plates w/uv 254. Column chromatography was carried out by a Biotage Isolera™ flash chromatography system, silica gel (E. Merck, 70–230 mesh) and sephadex LH-20 (Sigma- Aldrich chemical Co.) were used. All the reagents and solvents used for separation and purification were of analytical grade. For preparative isolation TLC silica gel 60 PR-18 F254S plates were used. Visualization of the TLC plates was achieved with a UV lamp (l = 254 and 365 nm), sprayed with Dragendorff's and anisaldehyde/acid spray reagent. All chemicals used were purchased from Sigma–Aldrich (St. Louis, Mo, USA). Three solvent systems were used for TLC analysis; S_1: ethyl acetate-methanol-ammonia sol. (95: 5: 2.5); S_2: dichloromethane-methanol (95: 5); S_3: methanol/water (70:30), The plates were dried and visualized under UV-light at 254 and 365 nm and sprayed with Dragendorff's and anisaldehyde/sulfuric acid spray reagents.

Table 4
Lowest energy conformers of papaverine and compounds (1–6).

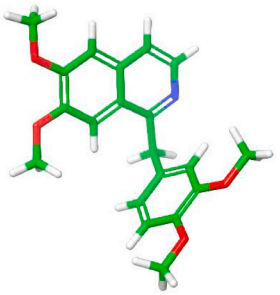	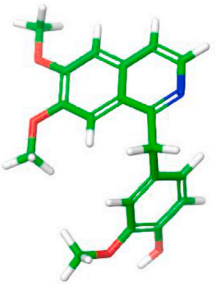	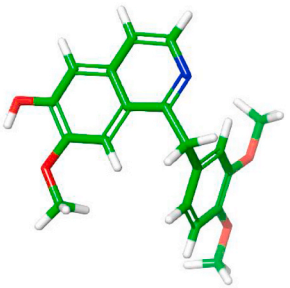
Papaverine OPLS3 energy 164.702 kJ/mol	(1) OPLS3 energy 117.608 kJ/mol	(2) OPLS3 energy 106.589 kJ/mol
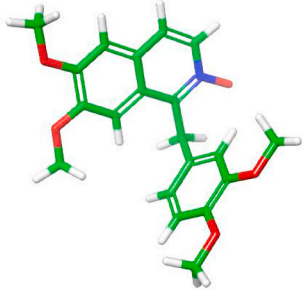	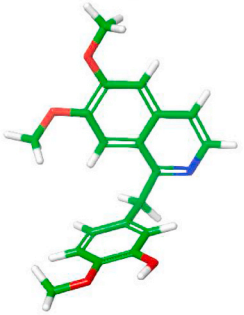	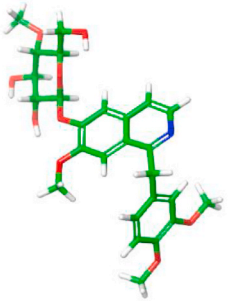
(3) OPLS3 energy 120.867 kJ/mol	(4) OPLS3 energy 101.369 kJ/mol	(5) OPLS3 energy 285.711 kJ/mol
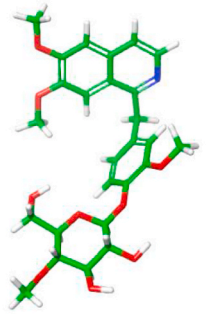		
(6) OPLS3 energy 285.079 kJ/mol		

Papaverine
OPLS3 energy 164.702 kJ/mol

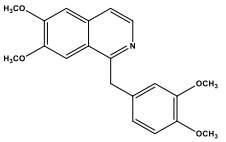

(1)
OPLS3 energy 117.608 kJ/mol

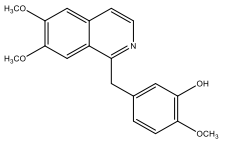

(2)
OPLS3 energy 106.589 kJ/mol

(*continued on next page*)

Table 4 (*continued*)

(3) OPLS3 energy 120.867 kJ/mol	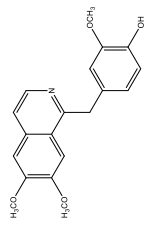
(4) OPLS3 energy 101.369 kJ/mol	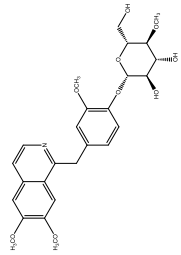
(5) OPLS3 energy 285.711 kJ/mol	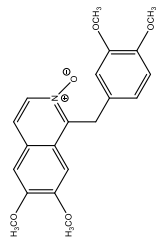
(6) OPLS3 energy 285.079 kJ/mol	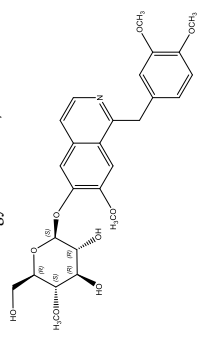

3.2. Chemicals

Papaverine was purchased from Sigma–Aldrich Inc. (Milwaukee, WI, USA).

3.3. Organism

Preliminary screening procedure were conducted as previously reported(Lee et al., 1990). Sixty microbial cultures, obtained from the University of Mississippi, NCNPR culture collection and twelve microbial cultures were obtained from the American Type Culture collection (ATCC, Rockville, Maryland), Northern Regional Research Laboratories (NRRL, Peoria, Illinois), USA. The cultures were initiated to grow from lyophilized state by adding 1 ml of sterile water to microorganism cells. Few drops of suspended cells were streaked on sabouraud-dextrose agar plates to check the purity. Pure cultures were maintained on slants of either potato-dextrose agar and sabouraud-dextrose agar. The fresh slants were incubated for few days at room temperature, before storage in a refrigerator (4 °C) and sub cultured every three months. On the basis of this screening process, several micro-organisms were found to metabolize papaverine very well with variable efficiencies without optimization. *Aspergillus niger* NRRL 322, *Beauveria bassiana* NRRL 22864, *Cunninghamella echinulate* ATCC 18968 and *Cunninghamella echinulate* ATCC 1382 were the most efficient microorganisms capable of conversion of Papaverine into metabolites.

The same procedure was used to produce large quantities of the metabolites. The highest yield microbial strains found to biotransform papaverine were chosen for the preparative-scale fermentation experiments. Papaverine (600 mg) dissolved in acetone and then equally divided among 2 L flasks containing 400 ml of stage II culture in a concentration of 10 mg/50 ml culture media (w/v). All fermentation experiments utilized a liquid media of the following composition: 20 g dextrose, 5 g yeast extract, 5 g K_2HPO_4, 5 g peptone and 5 g NaCl in 1 L of distilled water, which was sterilized at 121 °C for 15 min. After maximum conversion, the experiments were terminated and rendered alkaline with conc. Ammonium hydroxide (1 ml/30 ml culture, pH 8) then exhaustively extracted with equal volume of ethyl acetate, filtered off by a cheese cloth over anhydrous Na_2SO_4 and evaporated to dryness under vacuum using rotary evaporator to give fermentation residues.

3.4. Microbial transformation using Cunninghamella echinulate ATCC 18968

Biotransformation of papaverine using *Cunninghamella echinulate* ATCC 18968 produced one metabolite. The residue (800 mg) was dissolved in 30 ml of methanol/dichloromethane mixture (1:1) and adsorbed onto 800 mg Celite and dried. The adsorbed sample was placed onto a glass column (110 × 2 cm) packed with silica after making a slurry in dichloromethane. The column was gradiently eluted with dichloromethane 100% then dichloromethane: methanol (98.5:1.5, 98:2) and 10 ml fractions were collected. Fractions 40–60 were pooled together to give compound **1**. Further purification was achieved using sephadex LH-20 column, as determined by TLC. The metabolite was obtained in the form of white powder (70 mg, *Rf* 0.6 S_2).

3.5. Microbial transformation using Aspergillus niger NRRL 322

Biotransformation of papaverine using *Aspergillus niger* NRRL 322 afforded to two metabolites (2 and 3). The residue (1 gm) was dissolved in 50 ml of methanol/dichloromethane mixture (1:1) and adsorbed onto 1 gm Celite and dried. The adsorbed sample was placed onto a glass column (50 × 2.5 cm) packed with silica after making a slurry in dichloromethane. The column was isocratically eluted with dichloromethane: methanol (97.5:2.5) and 10 ml fractions were collected. Fractions 20–44 were pooled together to give mixture of **2** and **3** as determined by TLC. The metabolites were obtained in the form of

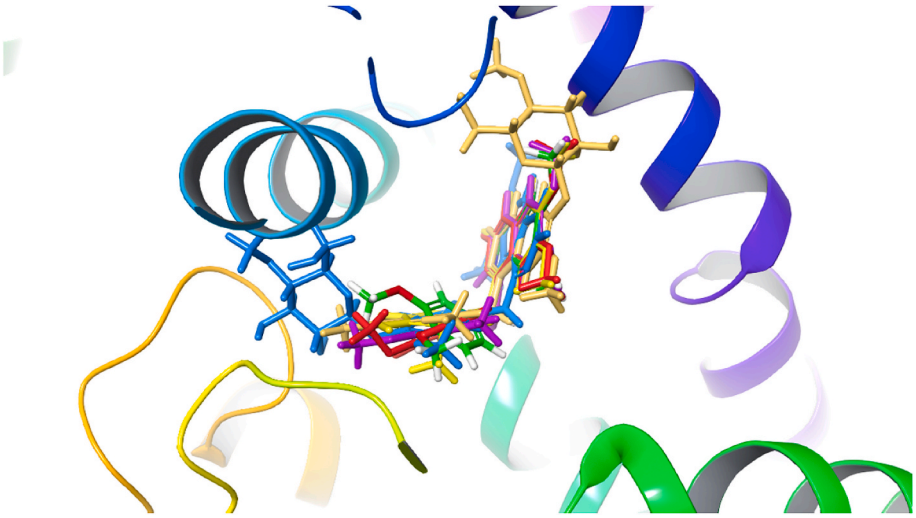

Fig. 2. Docked poses of the five papaverine-based biotransformation products with better docking scores than the native ligand in the Human PDE-10 A crystal structure, PDB: 2WEY; 4 (red), 1 (yellow), 6 (blue), 3 (blum), 5 (faded orange). (For interpretation of the references to colour in this figure legend, the reader is referred to the Web version of this article.)

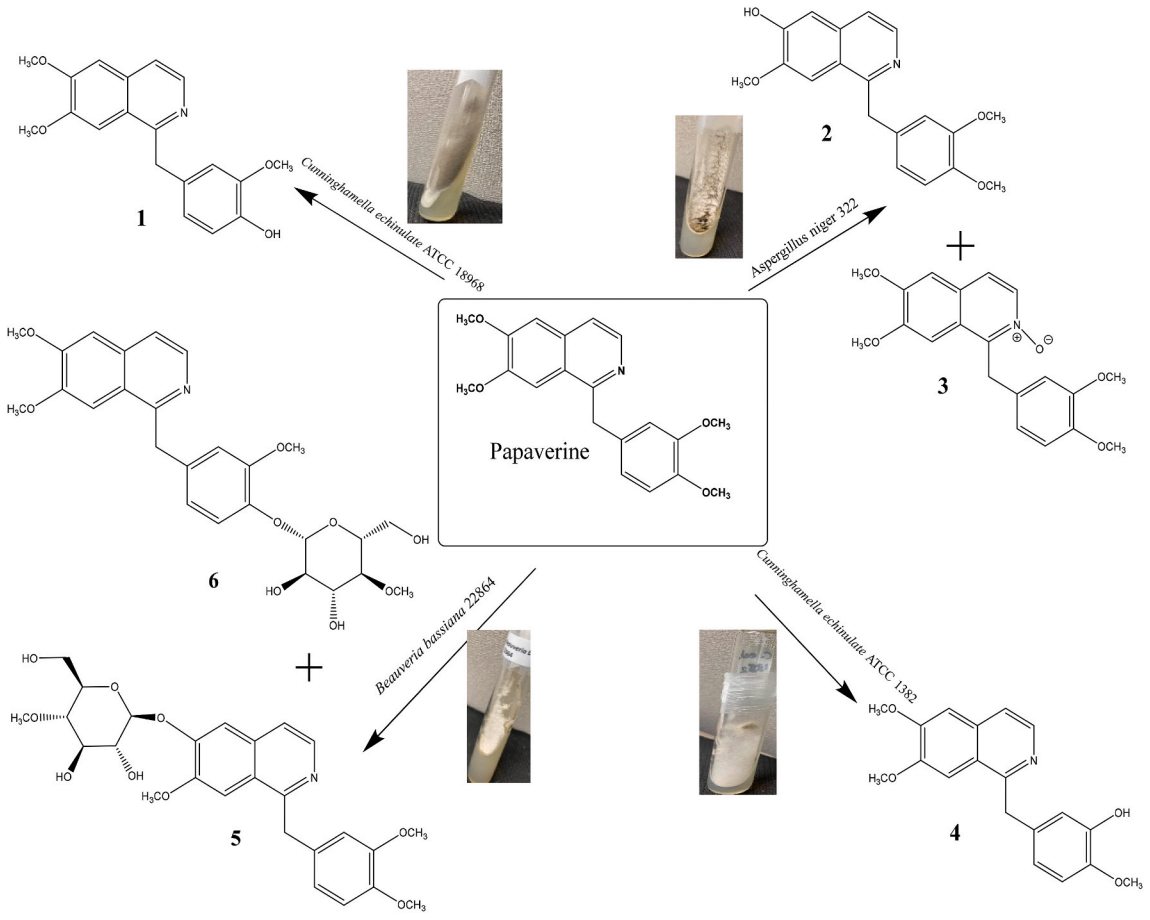

Fig. 3. Structure of papaverine and its metabolite from different Fungi.

yellowish residue (80 mg, *Rf* 0.3 S_2).

The mixture was loaded in silica biotage column (18 × 150 mm). The column was gradiently eluted with dichloromethane 100% then dichloromethane:2-propanol (98:2, 97:3,95:5) and 20 ml fractions were collected. Fractions 27–31 were pooled together to give pure **2**, in the form of white powder (7 mg, R_f 0.70 S_1). Fractions 65–85 were pooled together to give pure **3**, in the form of white powder (30 mg, *Rf* 0.61 S_1).

3.6. Microbial transformation using Cunninghamella echinulate ATCC 1382

Biotransformation of papaverine using *Cunninghamella echinulate* ATCC 1382 afforded to one metabolite. The residue (900 mg) was dissolved in 20 ml of methanol/dichloromethane mixture (1:1) and adsorbed onto 900 mg Celite and dried. The adsorbed sample was placed

Table 5
Docking scores of the biotransformation products in the binding site of 2WEY "Human PDE-papaverine complex".

Compound	Structure	Docking score	Glide score	Glide Emodel
Papaverine (native ligand)	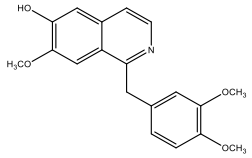	−5.335	−5.378	−36.528
4	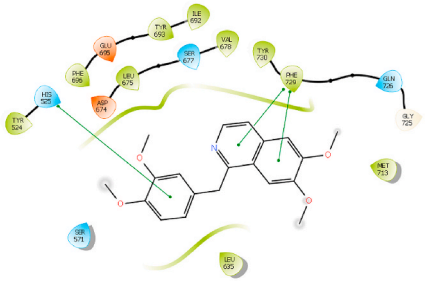	−6.610	−6.654	−57.572
1	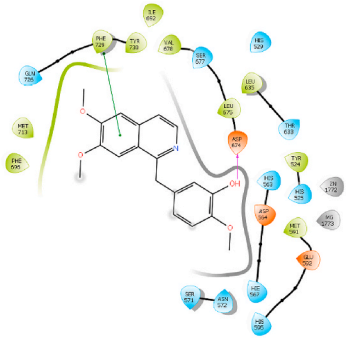	−6.305	−6.305	−47.271
6	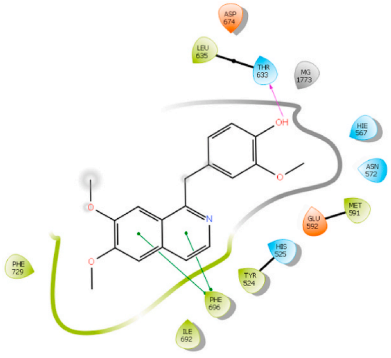	−6.213	−6.256	−59.876
3	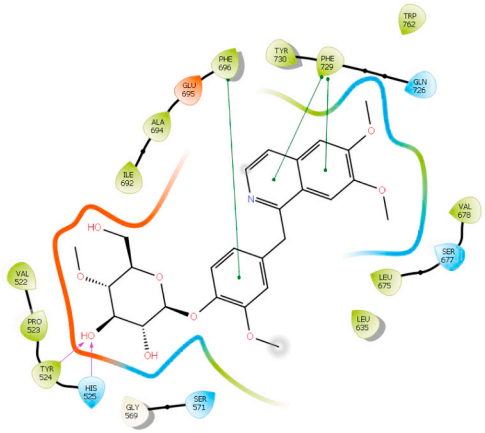	−6.128	−6.128	−37.724
5		−5.938	−6.109	−63.128

(*continued on next page*)

Table 5 (*continued*)

Compound	Structure	Docking score	Glide score	Glide Emodel
2	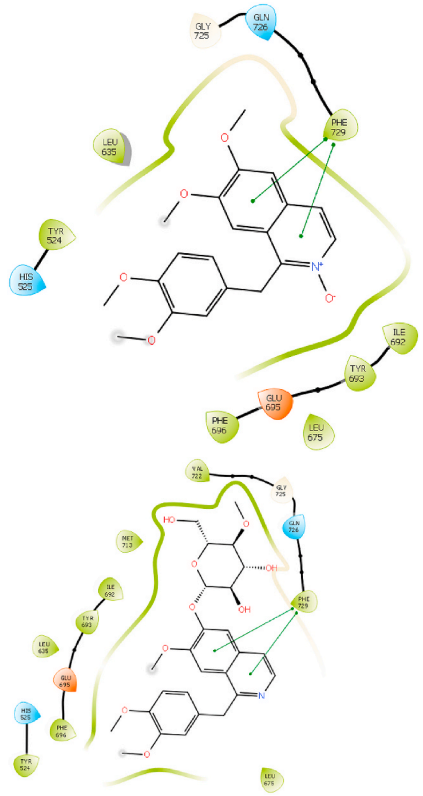	−4.834	−5.246	−48.062

onto a glass column (110 × 2.5 cm) packed with silica after making a slurry in dichloromethane. The column was gradiently eluted with dichloromethane 100% then dichloromethane: methanol (99.5:0.5, 99:1) and 20 ml fractions were collected. Fractions 50–75 were pooled together to give pure **4**, as determined by TLC. The metabolite was obtained in the form of white powder (8 mg, *Rf* 0.5 S_2).

3.7. Microbial transformation using Beauveria bassiana 22864

Biotransformation of papaverine using *Beauveria bassiana* 22864 afforded to two metabolites: **5** and **6**. The residue (1 g) was dissolved in 30 ml of methanol/dichloromethane mixture (1:1) and adsorbed onto 1 g Celite and dried. The adsorbed sample was placed onto a glass column (110 × 2.5 cm) packed with silica after making a slurry in dichloromethane. The column was gradiently eluted with dichloromethane: methanol (99:1, 95:5,94:6) and 10 ml fractions were collected. Fractions 50–119 were pooled together to give mixture of the two metabolites (80 mg), as determined by TLC. The two metabolites were separated by preparative silica gel 60 PR-18 plates (10 × 20 cm, 250 μm) (methanol: water, 70:30). 5 mg of the sample added in each plate. The bands were located using UV lamp then scratched and extracted using 100% methanol then evaporated, yielding to pure **5** in the form of white powder (5 mg, *Rf* 0.69 S_3) and pure **6** white powder (6 mg, *Rf* 0.61 S_3).

3.8. In silico molecular docking studies

3.8.1. Protein preparation

Crystal structure of Human PDE-papaverine complex 2WEY (Andersen et al., 2009) was downloaded from Protein Data Bank RCSB PDB (Berman et al., 2000). Chain A from the crystal structure was deleted since chain B contains the papaverine in the right binding mode (Andersen et al., 2009), followed by preprocessing to assign bond orders, use CCD database, add hydrogen bonds, create zero-order bonds to metals, create disulfide bonds, and delete water molecules beyond 5 Å from the hetero groups, generate het state using Epik at pH 7 ± 2. The H-bond assignment was applied using sample water orientations, using PROPKA pH 7.0. Water molecules with less than three hydrogen bonding distance were removed from the protein. Restrained minimization was performed using OPLS3, converged the heavy atoms to RMSD 0.3 Å.

3.8.2. Ligand preparation

Papaverine and compounds (1–6) were sketched in Maestro then prepared using LipPrep module (Schrödinger, LLC) in OPLS3 force field, generate possible states at target pH 7.0 ± 2 in Epik and generated tautomers. The specified chirality was retained to generate at most 32 per ligand. The structure from the previous step were minimizes using OPLS3 force field using Powell−Reeves conjugate gradient (PRCG) method with 2500 maximum iteration and gradient converge with 0.05 threshold. We have carried out the conformational searches using mixed torsional/low-mode sampling with 1000 maximum number of steps and 100 steps per rotatable bond. A 21 kJ/mol energy cutoff was used A conformer was considered redundant and subsequently eliminated if its maximum atom deviation from an already-identified conformer was less than 0.5.

3.8.3. Glide grid generation and docking

Receptor grid was generated for the prepared proteins 2WEY using Glide (Schrödinger, LLC). No constraints were applied. The grid thus generated was validated for the native ligands (papaverine) to check if the RMSD of the docked output was <1 Å from that of the crystal structure. All the generated conformers for the prepared ligands were docked in the generated grid. Their docking results and binding poses (table 6).

Table 6
Ligand-interaction diagram of compounds with key amino acid residues of Human PDE-10 A (PDB: 2WEY).

Papaverine	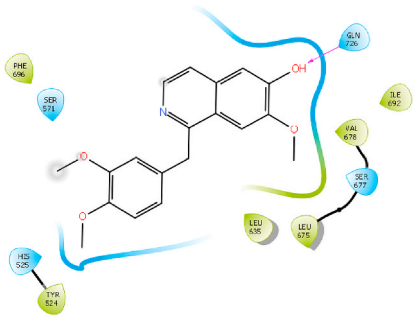
Compound 4	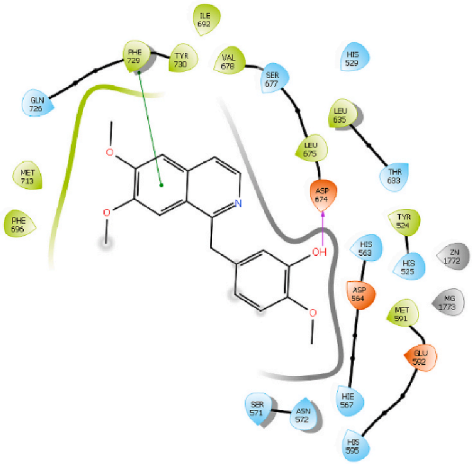
Compound 1	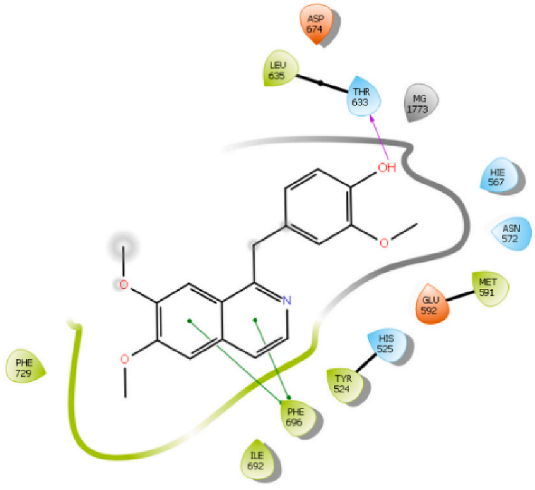
Compound 6	

(*continued on next page*)

Table 6 (*continued*)

Compound 3	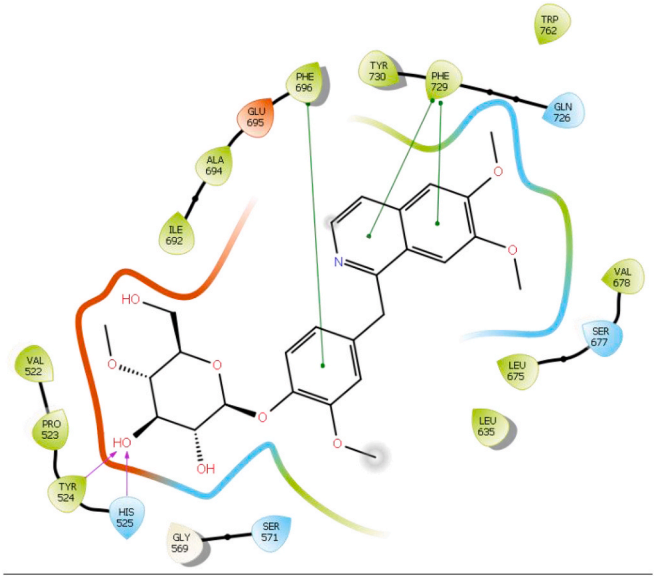
Compound 5	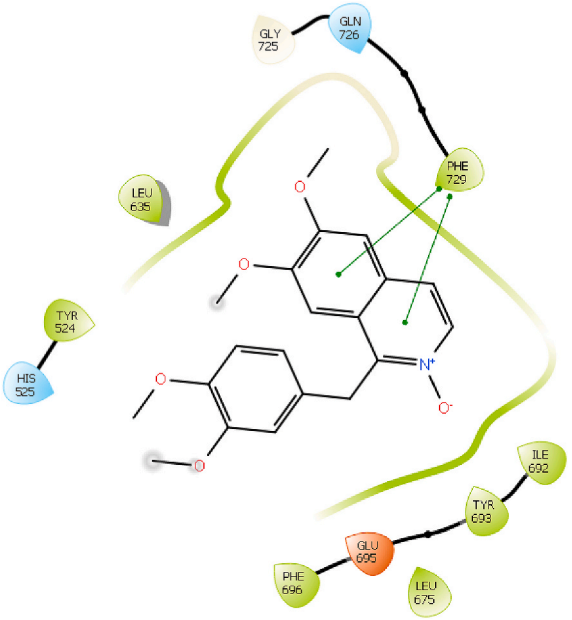
Compound 2	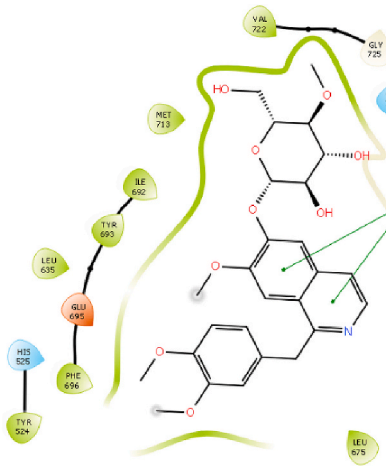

(*continued on next page*)

Table 6 (*continued*)

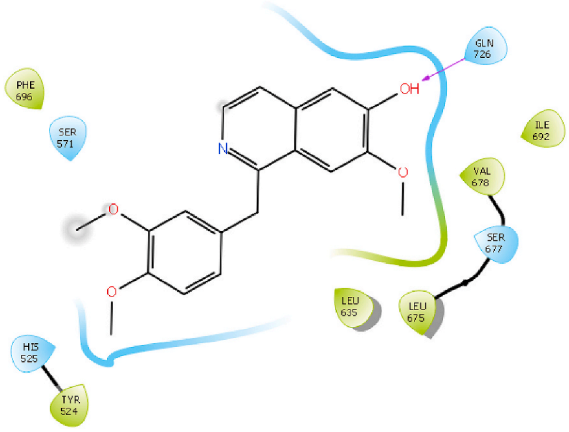

Declaration of competing interest

The authors declare that they have no known competing financial interests or personal relationships that could have appeared to influence the work reported in this paper.

Acknowledgments

The project was supported by the Egyptian government, National center of Natural product research, USA and in part by the USDA Agricultural Research Service.

References

Andersen, O., Schönfeld, D., Toogood-Johnson, I., Felicetti, B., Albrecht, C., Fryatt, T., Whittaker, M., Hallett, D., Barker, J., 2009. Cross-linking of protein crystals as an aid in the generation of binary protein-ligand crystal complexes, exemplified by the human PDE10a-papaverine structure. Acta Crystallogr. 65 (8), 872–874. https://doi.org/10.1107/S0907444909017855.

Belpaire, F., Bogaert, M., Rosseel, M., Anteunis, M., 1975. Metabolism of papaverine. I. Identification of metabolites in rat bile. Xenobiotica 5 (7), 413–420. https://dio.org:10.3109/00498257509056111.

Berman, H., Westbrook, J., Feng, Z., Gilliland, G., Bhat, T., Weissig, H., Shindyalov, I., Bourne, P., 2000. The protein Data Bank. Nucleic Acids Res. 28 (1), 235–242. https://doi.org/10.1093/nar/28.1.235.

Brochmann-Hanssen, E., Hirai, E., 1968. Opium Alkaloids VII. Isolation of a new benzylisoquinoline alkaloid. Synthesis and NMR Studies of papaveroline trimethyl ethers. J. Pharmaceut. Sci. 57 (6), 940–943. https://doi.org/10.1002/jps.2600570605.

Chen, S., Zhang, Y., Lighthouse, J.K., Mickelsen, D.M., Wu, J., Yao, P., Small, E.M., Yan, C., 2020. A novel role of cyclic nucleotide phosphodiesterase 10A in pathological cardiac remodeling and dysfunction. Circulation 141 (3), 217–233. https://doi.org/10.1161/CIRCULATIONAHA.119.042178.

Dorisse, P., Gleye, J., Loiseau, P., Puig, P., Edy, A., Henry, M., 1986. Papaverine biotransformation in plant cell suspension cultures. J. Nat. Prod. 51 (3), 532–536. https://doi.org/10.1021/np50057a013.

El Sayed, K., 2000. Microbial transformation of papaveraldine. Phytochemistry 53 (2000), 675–678. https://doi.org/10.1016/S0031-9422(99)00616-0.

Hagel, J., Facchini, P., 2013. Benzylisoquinoline alkaloid metabolism: a century of discovery and a brave new world. Plant Cell Physiol. 54 (5), 647–672. https://doi.org/10.1093/pcp/pct020.

Hegazy, M., Mohamed, T. ElShamy, Mahalel, U., Reda, E., Shaheen, A., Tawfik, W., Shahat, A., Shams, K., Abdel-Azim, N., Hammoud, F., 2015. Microbial biotransformation as a tool for drug development based on natural products from mevalonic acid pathway: a review. J. Adv. Res. 6 (1), 17–33. https://doi.org/10.1016/j.jare.2014.11.009.

Lee, I.-S., ElSohly, H.N., Hufford, C.D., 1990. Microbial metabolism studies of the antimalarial drug arteether. Pharmaceut. Res. 7 (2), 199–203. https://doi.org/10.1021/np50062a020.

Lee, Y., Park, J., Leem, Y., Park, J., Kim, D., Choi, Y., Park, E., Kang, J., Kim, H., 2019. The phosphodiesterase 10 inhibitor papaverine exerts anti-inflammatory and neuroprotective effects via the PKA signaling pathway in neuroinflammation and Parkinson's disease mouse models. J. Neuroinflammation 16 (1), 246. https://doi.org/10.1186/s12974-019-1649-3.

Li, J., Chen, J., Deng, Y., Zhou, Q., Wu, Y., Wu, D., Luo, H., 2018. Structure-based design, synthesis, biological evaluation, and molecular docking of novel PDE10 inhibitors with antioxidant activities. Frontiers in Chemistry 6, 167. https://doi.org/10.3389/fchem.2018.00167.

Salter, R., Beshore, D., Colletti, S., Evans, L., Gong, Y., Helmy, R., Liu, Yong, Maciolek, C., Martin, G., Pajkovic, N., Phipps, R., Small, J., Steele, J., de Vries, R., Williams, H., Martin, I., 2019. Microbial biotransformation – an important tool for the study of drug metabolism. Xenobiotica 49 (8), 877–886. https://doi.org/10.1080/00498254.2018.1512018.

Verdeil, L., Bister-Miel, F., Guignard, L., Viel, C., 1986. Papaverine biotransformation by *Silene alba* cell suspension. Planta Med. 1, 1–3. https://doi.org/10.1016/S0031-9422(00)84577-X.

Veeresham, C., Venisetty, R., 2003. Application of microbial biotransformation for the new drug discovery using natural drugs as substrates. Curr. Pharmaceut. Biotechnol. 4 (3), 153–167. https://doi.org/10.3389/fmicb.2015.01433.